

The impact of IGF-1 on alveolar bone remodeling and BMP-2 expression in orthodontic tooth movement in diabetic rats

Mengxi Wang^{1,D,E}, Yanfen Qiu^{2,A,F}, Lili Gao^{1,B}, Feng Qi^{1,D}, Liangjia Bi^{1,A,E}

¹ Department of Stomatology, The Fourth Affiliated Hospital of Harbin Medical University, China

² Department of Oral Radiology, School of Stomatology, Harbin Medical University, China

A – research concept and design; B – collection and/or assembly of data; C – data analysis and interpretation;

D – writing the article; E – critical revision of the article; F – final approval of the article

Advances in Clinical and Experimental Medicine, ISSN 1899–5276 (print), ISSN 2451–2680 (online)

Adv Clin Exp Med. 2023;32(3):349–356

Address for correspondence

Mengxi Wang
E-mail: nftphlnzl@sina.com

Funding sources

None declared

Conflict of interest

None declared

Received on July 27, 2018

Reviewed on May 14, 2022

Accepted on September 9, 2022

Published online on November 24, 2022

Abstract

Background. Orthodontic tooth movement is linked to alveolar bone reconstruction.

Objectives. As a regulator of cell proliferation, insulin-like growth factor 1 (IGF-1) plays an important role in osteoporotic fracture healing. This study aims to investigate the effect of IGF-1 on alveolar bone remodeling in diabetic rats.

Materials and methods. Sprague Dawley (SD) rats were randomly divided into 3 groups, including a control group, a model group established with streptozotocin (STZ) injection to prepare the diabetic rats (type 1 diabetes), and an IGF-1 group of diabetic rats receiving daily intraperitoneal injections of 1.0 mg/kg IGF-1. Nickel-titanium coil springs were used to pull the first molar forward to establish the model. The maxillary first to third molars and the surrounding alveolar bone were collected to measure tooth movement distance. Hematoxylin and eosin (H&E) staining was applied to detect the pathological changes in the periodontal tissue. Real-time polymerase chain reaction (PCR) and western blot were adopted to measure bone morphogenetic protein 2 (BMP-2) mRNA and protein expression. Enzyme-linked immunosorbent assays (ELISAs) were used to measure interleukin-1α (IL-1α) levels in the serum.

Results. The tooth movement distance was significantly decreased, BMP-2 expression was downregulated, and IL-1α levels were enhanced in the model group compared to the control group ($p < 0.05$). However, the tooth movement distance was increased, BMP-2 expression was increased, and IL-1α levels were reduced in the IGF-1 group compared to the model group ($p < 0.05$). Hematoxylin and eosin staining showed that alveolar bone destruction was attenuated in the IGF-1 group, while the new bone was not active in the model group.

Conclusions. Diabetes can damage alveolar bone remodeling in orthodontic tooth movement. The IGF-1 promotes alveolar bone remodeling by inhibiting inflammation and upregulating BMP-2 expression.

Key words: diabetes mellitus, IGF-1, BMP-2, alveolar bone remodeling, IL-1α

Cite as

Wang M, Qiu Y, Gao L, Qi F, Bi L. The impact of IGF-1 on alveolar bone remodeling and BMP-2 expression in orthodontic tooth movement in diabetic rats. *Adv Clin Exp Med.* 2023;32(3):349–356. doi:10.17219/acem/153956

DOI

10.17219/acem/153956

Copyright

Copyright by Author(s)

This is an article distributed under the terms of the Creative Commons Attribution 3.0 Unported (CC BY 3.0) (<https://creativecommons.org/licenses/by/3.0/>)

Background

The teeth are fixed in the alveolar fossa by attaching to the alveolar bone via the periodontal ligament. The orthodontic process is aimed at the correction of teeth and removal of malocclusions, and depends on the usage of correction devices inside or outside the mouth.^{1,2} It adjusts dental deformities and coordinates facial bone, maxillofacial, teeth, nerve, and muscle realignment. Moreover, it corrects the abnormal state between the upper and lower teeth, the upper and lower jaw, the teeth and the jaws, as well as the nerves and muscles, to ensure the balance, stability and beauty of the stomatognathic system.^{3,4} Through a corrective force on the teeth, alveolar bone and jaw, the device makes the misaligned teeth physically move to achieve a normal alignment and more natural beauty.⁵ People in many countries are more and more aware of the importance of aesthetic teeth and oral health, as a consequence the number of orthodontic patients continues to rise year after year.⁶ Alveolar bone reconstruction is critical in orthodontic tooth movement and the simultaneous changes in periodontal tissue caused by the tooth movement.^{6,7} Identifying the key factors in alveolar bone remodeling is beneficial in accelerating the orthodontic process. Acceleration of alveolar bone remodeling can be assisted by surgery, drugs and other treatment strategies.⁸ Periodontal disease, caries and other risks may escalate due to factors such as difficult physiological transformation, poor regeneration ability, and longer time required for adult alveolar bone reconstruction.^{9,10} Therefore, speeding up orthodontic tooth movement and shortening the orthodontic treatment time is crucial.

Diabetes mellitus (DM) can lead to metabolic disorders of minerals, in which increased blood glucose further aggravates vitamin, bone and other metabolic disorders.¹¹ A deficiency of insulin-like growth factor 1 (IGF-1) and other growth factors induces a variety of diabetic complications.^{12,13} Diabetes mellitus causes delayed union of the fracture, mainly due to the occurrence of diabetic osteopenia, which further increases the difficulty of adult orthodontics.¹⁴ Insulin-like growth factor 1 is an important bioactivity factor that plays an important role in the healing of osteoporotic fractures.^{15,16} However, the effect of IGF-1 on alveolar bone remodeling and bone morphogenetic protein 2 (BMP-2) expression in orthodontic tooth movement in diabetic rats has not been reported.

Objectives

Through establishing a type 1 diabetic rat model, this study investigated the influence of IGF-1 on alveolar bone remodeling.

Materials and methods

Experimental animals

A total of 60 healthy male Sprague Dawley (SD) rats at 3 months of age and weighing 250 ± 30 g were acquired from the experimental animal center at the Harbin Medical University, China. The feeding conditions included a temperature of $21 \pm 1^\circ\text{C}$, humidity of 50–70%, and a 12-hour day/night cycle.

The experiments on rats used for the experiments were approved by the Animal Ethics Committee of the Forth Affiliated Hospital of Harbin Medical University, China (approval No. ZWLLSC-08).

Main reagents and instruments

Streptozotocin (STZ) was purchased from Sigma-Aldrich (St. Louis, USA). Trizol reagents were bought from Invitrogen (Shanghai, China). Polyvinylidene fluoride (PVDF) membranes were obtained from Pall Life Sciences Inc. (Port Washington, USA). Western blot-related chemical reagents were obtained from Beyotime (Shanghai, China). Enhanced chemiluminescence (ECL) reagents were provided by Amersham Biosciences (Amersham, UK). Mouse anti-rat BMP-2 monoclonal antibodies and goat anti-mouse horseradish peroxidase (HRP)-labeled immunoglobulin G (IgG) secondary antibodies were purchased from Cell Signaling Technology (Danvers, USA). The RNA extraction kits and reverse transcription kits were bought from Axygen (Union City, USA). Interleukin-1 α (IL-1 α) enzyme-linked immunosorbent assay (ELISA) kits were obtained from R&D Systems (Minneapolis, USA). Rat urine protein detection reagents were obtained from Beijing Furu Bioengineering Company (Beijing, China). The Lab-system v. 1.3.1 microplate reader was provided by Bio-Rad Laboratories (Hercules, USA). The ABI 7700 Fast Fluorescence Quantitative PCR was purchased from ABI (Foster City, USA). The DNA amplifier PE Gene Amp PCR System 2400 was purchased from Perkin Elmer (Waltham, USA). An electronic blood glucose meter was purchased from Advantage (Indianapolis, USA). Surgical equipment was purchased from the Suzhou Medical Equipment Factory (Suzhou, China). A surgical microscope was bought from the Jiangsu Zhenjiang Optical Instrument Company (model LZL-21; Zhenjiang, China). Automatic Biochemistry Analyzer BK-200 (Shandong Boke Biological Industry, Jinan, China) was used. Urine glucose test paper was obtained from the Pearl River Biochemical Reagents Company (Guangzhou, China). Other commonly used reagents were purchased from Sangon Biotech (Shanghai, China).

Grouping

Sixty SD rats were randomly and equally divided into 3 groups, including a control group, a model group

established by injecting STZ to prepare a diabetic rat, and an IGF-1 group, in which diabetic rats received daily intraperitoneal injections of 1.0 mg/kg IGF-1.

DM model preparation

Diabetes mellitus rats were used for modeling after adaptive breeding for 1 week. The rats fasted for 12 h and received 1% STZ solution as a single intraperitoneal injection using a dose of 60 mg/kg. Blood and urine glucose levels were tested after 48 h. Blood glucose > 16.7 mmol/L and urine glucose above +++ (>55.0 mmol/L) were considered successful modeling.¹⁷

Establishment of rat orthodontics model

The rats were anesthetized with 10% chloral hydrate via intraperitoneal injection and fixed. Next, a 0.2-mm concavity was ground into the distal axis angle of bilateral upper jaws, the lips, the tongue, and the gingival margin between the mesial surface of the first molar and the axial angle. Nickel-titanium coil springs were measured for the initial length out of the mouth and remeasured within the mouth after force proofing to ensure their accuracy. Then, the coil springs were fixed in the concave by a 0.2-mm ligation wire and 50 g of force was added to both sides to pull the first molar forward.¹⁸

Specimen collection

The rats were euthanized on the 16th day after treatment. Aorta blood was collected and stored at room temperature for 30 min. Then, the blood was centrifuged at 3600 rpm for 10 min at 4°C and the serum was stored at -20°C. The specimens of bilateral maxillary first to third molars and surrounding alveolar bone were collected and fixed in 4% paraformaldehyde for 24 h. After measuring the distance of the experimental tooth movement, the specimens were decalcified using a 10% ethylenediaminetetraacetic acid (EDTA) solution.

ELISA

Enzyme-linked immunosorbent assay was used to test IL-1 α content in the supernatant. A total of 50 μ L of diluted standard substance were added into each well to establish a standard curve. Next, a 50- μ L sample was added to the plate and washed 5 times. Then, 50 μ L of conjugate reagent were added and incubated at 37°C for 30 min. After being washed 5 times, 50 μ L of color agents A and B were added and incubated at 37°C for 30 min in the dark, followed by the addition of 50 μ L of buffer to stop the reaction and subsequent measurement of the optical density (OD) value at a wavelength of 450 nm. The OD value of the standard substance was used to prepare the linear regression

equation, which was adopted to calculate the concentration of samples.

Real-time PCR

Total RNA was extracted from alveolar bone and reversely transcribed into cDNA. The primers were designed using Primer Premier v. 6.0 software (PREMIER Biosoft, San Francisco, USA) based on the mRNA sequence (BMP-2: accession number: NM_017178.1 and glyceraldehyde-3-phosphate dehydrogenase (GAPDH): accession number: NM_017008.4) and synthesized by Invitrogen (Table 1). Using SYBR Green qPCR SuperMix, the real-time polymerase chain reaction (PCR) was performed at 56°C for 1 min, followed by 35 cycles at 92°C for 30 s, 35 cycles at 58°C for 45 s, and 35 cycles at 72°C for 35 s. Glyceraldehyde-3-phosphate dehydrogenase was selected as an internal reference. The relative expression of mRNA was calculated using the $2^{-\Delta\Delta CT}$ method.

Table 1. Primer sequences

Gene	Forward 5'-3'	Reverse 5'-3'
GAPDH	AGTACCAGTCTGTTGCTGG	TAATAGACCCGGATGTCTGGT
BMP-2	TGCACCTACTCTCGATCCAT	GTGTAGGACCTCATACCTT

Western blot

Radioimmunoprecipitation assay (RIPA) lysis buffer was added to the alveolar bone and cracked on ice for 15–30 min. Next, the tissue was treated 4 times with ultrasound lasting 5 s, and centrifuged at 10,000 g for 15 min. The protein was transferred to a new Eppendorf (Ep) tube and quantified using the Bradford method. The protein was separated using 10% sodium dodecyl sulfate-polyacrylamide gel electrophoresis (SDS-PAGE) and transferred to a PVDF membrane using 100 mA for 1.5 h. After blocking with 5% skim milk for 2 h, the membrane was incubated with BMP-2 antibodies (1:2000) at 4°C overnight. Then, the membrane was incubated with HRP-conjugated goat anti-rabbit secondary antibody (1:2000) at room temperature for 30 min. After that, the ECL reagent was added to the membrane and incubated for 1 min, followed by exposure. The film was scanned using Quantity One software (Bio-Rad Laboratories) and analyzed with a protein image processing system. Four independent experiments were performed for each assay.

Hematoxylin and eosin staining

The alveolar bone tissue was decalcified in 10% EDTA, dehydrated in ethanol, dewaxed with xylene, embedded in paraffin, and stained with hematoxylin and eosin (H&E). At last, the samples were observed under a light microscope (Olympus BX51; Olympus Corp., Tokyo, Japan).

Statistical analyses

The R software package v. 3.6.1 (R Foundation for Statistical Computing, Vienna, Austria) was used for statistical analyses of all the data, and the Shapiro–Wilk test was used to evaluate the normality of the data. The results were shown in Supplementary Table 1. A value of $p > 0.05$ indicates that the orthodontic tooth movement distance, BMP-2 mRNA expression, BMP-2 protein expression, and serum IL-1 α levels all conformed to a normal distribution and are expressed as a mean \pm standard deviation. In addition, the Levene's test was consistent with the homogeneity of variance of normally distributed data; the results of the Levene's test are shown in Supplementary Table 2. One-way analysis of variance (ANOVA) and the Tukey's post hoc test were used to compare the differences between the groups, degrees of freedom (df) = K–1, where K is the number of groups. The p-value smaller than 0.05 indicated statistically significant differences between the groups.

Results

Orthodontic tooth movement distance

The comparison results of orthodontic tooth movement distances are shown in Fig. 1 and Table 2. Under the action of orthodontic force, the tooth movement distance of the 3 groups gradually increased. A comparison of tooth movement distances between the control group, model group and IGF-1 group was performed using ANOVA and Tukey's post hoc test. The results showed that $F = 389.40$, $p < 0.001$, $df = 2$, and the difference between the 3 groups was statistically significant. The results of the Tukey's post hoc tests are shown in Supplementary Table 3. The tooth movement distance in the model group (0.3 ± 0.06 mm) was significantly shorter than in the control group (0.8 ± 0.05 mm, $p < 0.001$). Compared to the model group, the distance in the IGF-1 group significantly increased (0.62 ± 0.06 mm, $p < 0.001$). The tooth movement distance in the IGF-1 group was significantly shorter than in the control group ($p < 0.001$).

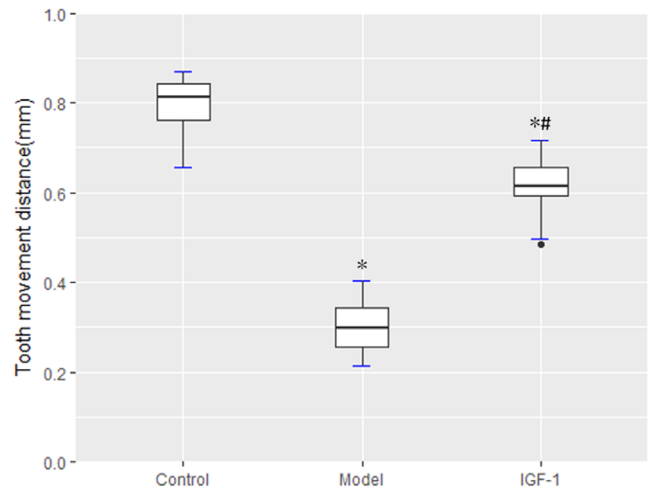


Fig. 1. Orthodontic tooth movement distance. Comparison between the model group and the control group, * $p < 0.001$; the insulin-like growth factor 1 (IGF-1) group and the control group, * $p < 0.001$; the IGF-1 group compared with the model group, # $p < 0.001$. The upper and lower boundaries of the main body of the box diagram are the upper and the lower quartile, the horizontal line in the middle is the median, the whiskers extend to a maximum of $1.5 \times$ interquartile range (IQR) beyond the box, and the black dots represent outliers

Histological analysis with H&E staining

The rats in each group showed periodontal membrane narrowing and alveolar bone resorption on the pressure side. Increased bone deposits and new bone formation were found in the bone resorption pit on the tension side of the control group. The number of osteoclasts increased in the model group. Osteoclasts were decreased in the IGF-1 group and the periodontal and dental tissue began to repair. A small number of osteoblasts were seen arranged in the IGF-1 group (Fig. 2).

BMP-2 mRNA expression

Real-time PCR was used to detect BMP-2 mRNA expression in rat alveolar bone, and the results are shown in Fig. 3 and Table 3. The BMP-2 mRNA expression levels in the control group, model group and IGF-1 group were compared using one-way ANOVA and Tukey's post hoc test ($F = 270.52$, $p < 0.001$, $df = 2$), and the differences among the 3 groups were statistically significant. The results of the Tukey's post hoc test are shown in Supplementary Table 4. The BMP-2 mRNA expression in the model

Table 2. Orthodontic tooth movement distance

Group	n	Orthodontic tooth movement distance [mm]	F	df	p-value
Control group	20	0.80 ± 0.05	389.395	2	<0.001
Model group	20	0.30 ± 0.06			
IGF-1 group	20	0.62 ± 0.06			

IGF-1 – insulin-like growth factor 1; df – degrees of freedom.

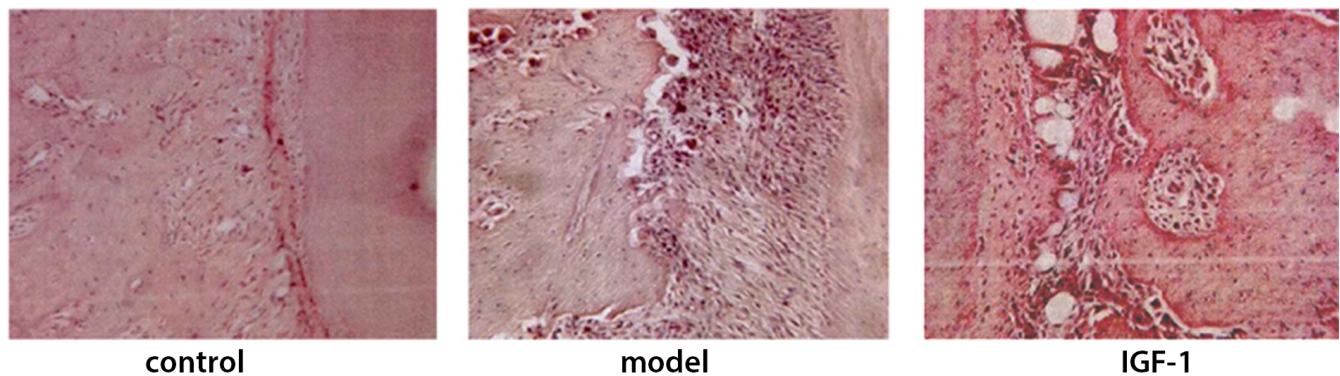


Fig. 2. Histological changes observed using hematoxylin and eosin (H&E) staining (x200 magnification)

IGF-1 – insulin-like growth factor 1.

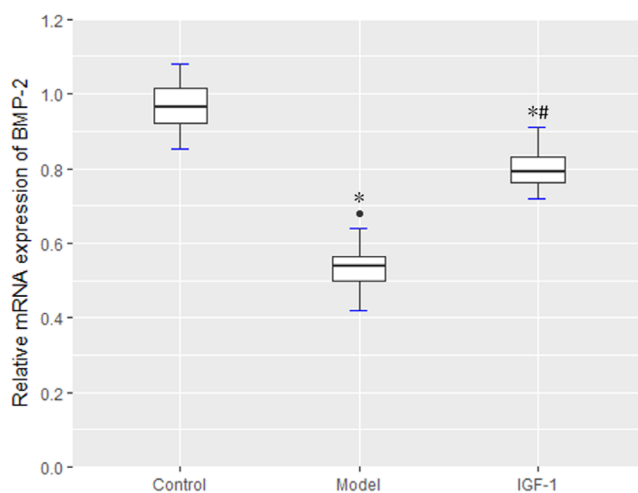


Fig. 3. Bone morphogenetic protein 2 (BMP-2) mRNA expression changes. Comparison between the model group and the control group, * $p < 0.001$; the insulin-like growth factor 1 (IGF-1) group and the control group, * $p < 0.001$; the IGF-1 group and the model group, * $p < 0.001$. The upper and lower boundaries of the main body of the box diagram are the upper and the lower quartile, the horizontal line in the middle is the median, the whiskers extend to a maximum of $1.5 \times$ interquartile range (IQR) beyond the box, and the black dots represent outliers

group (0.53 ± 0.06) was significantly lower than in the control group (0.96 ± 0.06 , $p < 0.001$). However, compared with the model group, BMP-2 mRNA expression in the IGF-1 group was significantly increased (0.8 ± 0.05 , $p < 0.001$), and the BMP-2 mRNA expression in the IGF-1 group was significantly lower than in the control group ($p < 0.001$).

BMP-2 protein expression

Western blot was used to detect the expression of BMP-2 protein in rat alveolar bone, and the results are presented in Fig. 4 and Table 4. The expression levels of BMP-2 protein in the control group, model group and IGF-1 group were compared using one-way ANOVA and Tukey's post hoc test ($F = 224.54$, $p < 0.001$, $df = 2$), and the differences among the 3 groups were statistically significant. The results of the Tukey's post hoc test are shown in Supplementary Table 5. The expression of BMP-2 protein in the model group (0.72 ± 0.07) was significantly lower than in the control group (1.20 ± 0.08 , $p < 0.001$). However, BMP-2 protein expression in the IGF-1 group (0.91 ± 0.06) was significantly higher than in the model group ($p < 0.001$), and in the IGF-1 group it was significantly lower than in the control group ($p < 0.001$).

Table 3. BMP-2 mRNA expression changes

Group	n	BMP-2 mRNA expression changes	F	df	p-value
Control group	20	0.96 ± 0.06	270.520	2	<0.001
Model group	20	0.53 ± 0.06			
IGF-1 group	20	0.80 ± 0.05			

IGF-1 – insulin-like growth factor 1; df – degrees of freedom; BMP-2 – bone morphogenetic protein 2.

Table 4. BMP-2 protein expression changes

Group	n	BMP-2 protein expression changes	F	df	p-value
Control group	20	1.20 ± 0.08	224.542	2	<0.001
Model group	20	0.72 ± 0.07			
IGF-1 group	20	0.91 ± 0.06			

IGF-1 – insulin-like growth factor 1; df – degrees of freedom; BMP-2 – bone morphogenetic protein 2.

Table 5. Serum IL-1 α levels

Group	n	Serum IL-1 α levels [pg/mL]	F	df	p-value
Control group	20	107.86 \pm 26.66	242.797	2	<0.001
Model group	20	276.11 \pm 23.26			
IGF-1 group	20	217.21 \pm 23.44			

IL-1 α – interleukin-1 α ; IGF-1 – insulin-like growth factor 1; df – degrees of freedom.

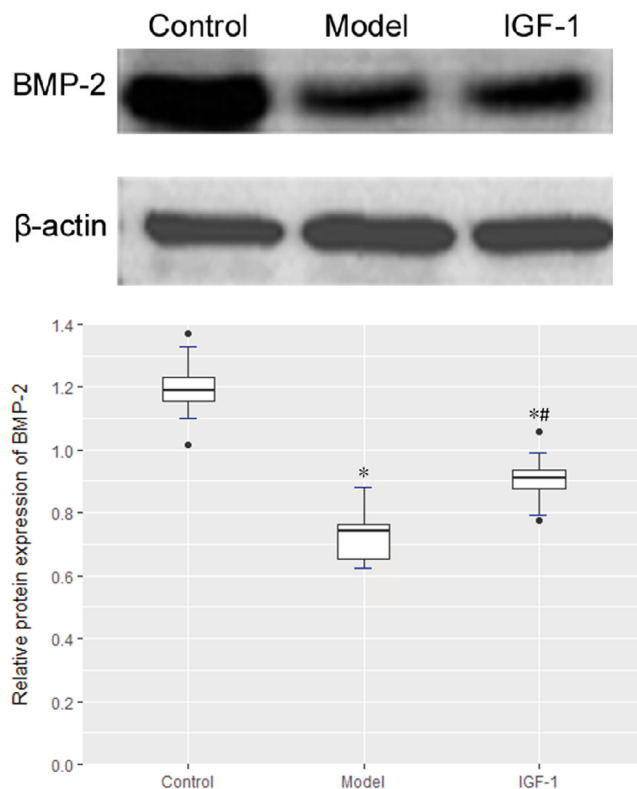


Fig. 4. Bone morphogenetic protein 2 (BMP-2) expression changes. Comparison between the model group and the control group, * $p < 0.004$; the insulin-like growth factor 1 (IGF-1) group and the control group, * $p < 0.001$; the IGF-1 group and the model group, # $p < 0.001$. The upper and lower boundaries of the main body of the box diagram are the upper and the lower quartile, the horizontal line in the middle is the median, the whiskers extend to a maximum of 1.5 \times interquartile range (IQR) beyond the box, and the black dots represent outliers

The expression of IL-1 α in serum

The expression of IL-1 α in serum was detected with ELISA, and the results were shown in Fig. 5 and Table 5. The serum IL-1 α levels of the control group, model group and IGF-1 group were compared using one-way ANOVA and Tukey's post hoc test ($F = 242.80$, $p < 0.001$, $df = 2$), and the differences among the 3 groups were statistically significant. The results of the Tukey's post hoc test are shown in Supplementary Table 6. The serum IL-1 α levels in the model group (276.11 ± 23.26 pg/mL) were significantly higher than in the control group (107.86 ± 26.66 pg/mL, $p < 0.001$). The level of IL-1 α in the IGF-1 group was 217.21 ± 23.44 pg/mL, which was significantly lower than in the model group ($p < 0.001$).

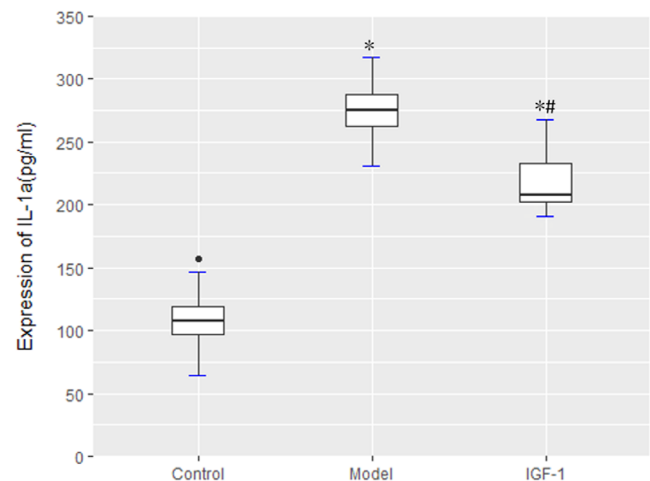


Fig. 5. Serum interleukin-1 α (IL-1 α) levels. Comparison between the model group and the control group, * $p < 0.001$; the IGF-1 group and the control group, * $p < 0.001$; the IGF-1 group and the model group, # $p < 0.001$. The upper and lower boundaries of the main body of the box diagram are the upper and the lower quartile, the horizontal line in the middle is the median, the whiskers extend to a maximum of 1.5 \times interquartile range (IQR) beyond the box, and the black dots represent outliers

The level of IL-1 α in the IGF-1 group was significantly higher than in the control group ($p < 0.001$).

Discussion

Reduced physical activity and overeating can cause endocrine and metabolic disorders, resulting in the occurrence and development of DM. Diabetes mellitus causes damage to multiple tissues and organs and induces microvascular disease, as well as cardiovascular and cerebrovascular diseases, which seriously affect the prognosis. Diabetes mellitus is an enormous challenge faced by the endocrine disciplines.¹⁹ On the other hand, DM-induced metabolic disorders, increased blood glucose, and insulin deficiency further aggravate abnormal bone metabolism, leading to osteoporosis which affects orthodontics.²⁰ This study showed a reduced distance of tooth movement and formed bone resorption lacunae, an increased number of osteoclasts, as well as enhanced secretion of IL-1 α during the orthodontic process in DM rats. These factors affect orthodontic tooth movement during alveolar bone reconstruction.

The IGF-1, also known as somatostatin C, is regulated by pituitary growth hormone together with growth

hormone C. The IGF-1 is synthesized and secreted by osteoblasts, osteoclasts and other cells.²¹ It regulates bone metabolism by binding to receptors on the surface of specific target cells mainly through autocrine and paracrine pathways. It induces bone marrow stromal cells and osteoblast differentiation, and promotes the synthesis of type I collagen fibers that can promote differentiation, leading to the facilitation of bone metabolism.²² Therefore, this study explored the role of IGF-1 during the orthodontic process in DM rats and showed that IGF-1 accelerated the movement of teeth, promoted new bone formation, reduced the number of osteoclasts, and inhibited the secretion of inflammatory factors resulting in enhanced reconstruction of alveolar bone during orthodontic tooth movement. Further investigations found that IGF-1 increased BMP-2 mRNA and protein expression. It has been proven that BMP-2 plays an important role in the process of fracture healing. The BMP-2 promotes the expression of bone matrix proteins by regulating bone alkaline phosphatase, thereby contributing to the mineralization of the extracellular matrix and the promotion of the orthodontics process.^{23,24}

Limitations

This study has some limitations. Although the role of IGF-1 in orthodontic alveolar bone remodeling in DM rats has been demonstrated, the exact molecular mechanisms by which IGF-1 is involved in alveolar bone remodeling in DM require further investigations. In addition, whether IGF-1 plays a role in alveolar bone remodeling in DM patients needs to be verified.

Conclusions

Diabetes mellitus destroys alveolar bone remodeling in orthodontic tooth movement and IGF-1 promotes alveolar bone remodeling, possibly by promoting BMP-2 expression and inhibiting inflammation.

Supplementary data

The Supplementary data are available at <https://doi.org/10.5281/zenodo.7317395>. The package contains the following files:

Supplementary Table 1. Results of Shapiro–Wilk test.

Supplementary Table 2. Results of Levene's test.

Supplementary Table 3. Results of Tukey's post hoc test of orthodontic tooth movement distance.

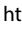
Supplementary Table 4. Results of Tukey's post hoc test of BMP-2 mRNA expression changes.

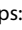
Supplementary Table 5. Results of Tukey's post hoc test of BMP-2 protein expression changes.


Supplementary Table 6. Results of Tukey's post hoc test of serum IL-1 α levels.

ORCID iDs

Mengxi Wang  <https://orcid.org/0000-0001-9709-3378>

Yanfen Qiu  <https://orcid.org/0000-0002-8955-2623>

Lili Gao  <https://orcid.org/0000-0001-6412-6516>

Feng Qi  <https://orcid.org/0000-0002-4863-6492>

Liangjia Bi  <https://orcid.org/0000-0001-9691-0903>

References

1. Arun M, Usman Q, Johal A. Orthodontic treatment modalities: A qualitative assessment of Internet information. *J Orthod*. 2017;44(2):82–89. doi:10.1080/14653125.2017.1313546
2. Al-Zoubi H, Alharbi AA, Ferguson DJ, Zafar MS. Frequency of impacted teeth and categorization of impacted canines: A retrospective radiographic study using orthopantomograms. *Eur J Dent*. 2017;11(1):117–121. doi:10.4103/ejd.ejd_308_16
3. Tehrani A, Motamedian SR, Saedi S, Kabiri S, Shidfar S. Correlation between frontal sinus dimensions and cephalometric indices: A cross-sectional study. *Eur J Dent*. 2017;11(1):64–70. doi:10.4103/1305-7456.202630
4. Saleh M, Hajeer MY, Muessig D. Acceptability comparison between Hawley retainers and vacuum-formed retainers in orthodontic adult patients: A single-centre, randomized controlled trial. *Eur J Orthod*. 2017;39(4):453–461. doi:10.1093/ejo/cjx024
5. Vicente A, Ortiz Ruiz AJ, González Paz BM, García López J, Bravo-González LA. Efficacy of fluoride varnishes for preventing enamel demineralization after interproximal enamel reduction: Qualitative and quantitative evaluation. *PLoS One*. 2017;12(4):e0176389. doi:10.1371/journal.pone.0176389
6. Yi J, Xiao J, Li Y, Li X, Zhao Z. Efficacy of piezocision on accelerating orthodontic tooth movement: A systematic review. *Angle Orthod*. 2017;87(4):491–498. doi:10.2319/01191-751.1
7. Li Y, Hu Z, Zhou C, et al. Intermittent parathyroid hormone (PTH) promotes cementogenesis and alleviates the catabolic effects of mechanical strain in cementoblasts. *BMC Cell Biol*. 2017;18(1):19. doi:10.1186/s12860-017-0133-0
8. Savoldi F, Visconti L, Dalessandri D, et al. In vitro evaluation of the influence of velocity on sliding resistance of stainless steel arch wires in a self-ligating orthodontic bracket. *Orthod Craniofac Res*. 2017;20(2):119–125. doi:10.1111/ocr.12156
9. Rashid A, ElSharaby FA, Nassef EM, Mehanni S, Mostafa YA. Effect of platelet-rich plasma on orthodontic tooth movement in dogs. *Orthod Craniofac Res*. 2017;20(2):102–110. doi:10.1111/ocr.12146
10. Angelieri F, Franchi L, Cevidanes LHS, Hino CT, Nguyen T, McNamara JA. Zygomaticomaxillary suture maturation: A predictor of maxillary protrusion? Part I. A classification method. *Orthod Craniofac Res*. 2017;20(2):85–94. doi:10.1111/ocr.12143
11. Mostafavinia A, Ahadi R, Abdollahifar M, Ghorishi SK, Jalalifiroozkhouhi A, Bayat M. Evaluation of the effects of photobiomodulation on biomechanical properties and Hounsfield unit of partial osteotomy healing in an experimental rat model of type I diabetes and osteoporosis. *Photomed Laser Surg*. 2017;35(10):520–529. doi:10.1089/pho.2016.4191
12. Canda MT, Demir N, Sezer O. Fetal nasal bone length as a novel marker for prediction of adverse perinatal outcomes in the first trimester of pregnancy. *Balkan Med J*. 2017;34(2):127–131. doi:10.4274/balkan-medj.2016.0133
13. Mishra R, Cano E, Venkatram S, Diaz-Fuentes G. An interesting case of mycoplasma pneumonia associated multisystem involvement and diffuse alveolar hemorrhage. *Respir Med Case Rep*. 2017;21:78–81. doi:10.1016/j.rmcr.2017.03.022
14. Raška I, Rašková M, Zikán V, Škrha J. Prevalence and risk factors of osteoporosis in postmenopausal women with type 2 diabetes mellitus. *Cent Eur J Public Health*. 2017;25(1):3–10. doi:10.21101/cejph.a4717
15. Ogundele OM, Ebenezer PJ, Lee CC, Francis J. Stress-altered synaptic plasticity and DAMP signaling in the hippocampus-PFC axis: Elucidating the significance of IGF-1/IGF-1R/CaMKII α expression in neural changes associated with a prolonged exposure therapy. *Neuroscience*. 2017;353:147–165. doi:10.1016/j.neuroscience.2017.04.008
16. Weischendorf S, Kielsen K, Sengeløv H, et al. Associations between levels of insulin-like growth factor 1 and sinusoidal obstruction syndrome after allogeneic haematopoietic stem cell transplantation. *Bone Marrow Transplant*. 2017;52(6):863–869. doi:10.1038/bmt.2017.43

17. Hazell TJ, Olver TD, Kowalchuk H, et al. Aerobic endurance training does not protect bone against poorly controlled type 1 diabetes in young adult rats. *Calcif Tissue Int.* 2017;100(4):374–381. doi:10.1007/s00223-016-0227-2
18. Faienza MF, Ventura A, Delvecchio M, et al. High sclerostin and Dickkopf-1 (DKK-1) serum levels in children and adolescents with type 1 diabetes mellitus. *J Clin Endocrinol Metab.* 2017;102(4):1174–1181. doi:10.1210/jc.2016-2371
19. Domouky AM, Hegab AS, Al-Shahat A, Raafat N. Mesenchymal stem cells and differentiated insulin producing cells are new horizons for pancreatic regeneration in type I diabetes mellitus. *Int J Biochem Cell Biol.* 2017;87:77–85. doi:10.1016/j.biocel.2017.03.018
20. Pogliacomi F, Pellegrini A, Tacci F, et al. Risks of subsequent contralateral fractures of the trochanteric region in elderly. *Acta Biomed.* 2016;87(3):275–281. PMID:28112694.
21. Mehrpour M, Rahatlou H, Hamzehpur N, Kia S, Safdarian M. Association of insulin-like growth factor-I with the severity and outcomes of acute ischemic stroke. *Iran J Neurol.* 2016;15(4):214–218. PMID:28435630.
22. Shahbazi M, Abdolmohammadi R, Ebadi H, Farazmandfar T. Novel functional polymorphism in *IGF-1* gene associated with multiple sclerosis: A new insight to MS. *Multiple Scler Relat Dis.* 2017;13:33–37. doi:10.1016/j.msard.2017.02.002
23. Dohan Ehrenfest DM, Pinto NR, Pereda A, et al. The impact of the centrifuge characteristics and centrifugation protocols on the cells, growth factors, and fibrin architecture of a leukocyte- and platelet-rich fibrin (L-PRF) clot and membrane. *Platelets.* 2018;29(2):171–184. doi:10.1080/09537104.2017.1293812
24. López-Cebral R, Civantos A, Ramos V, et al. Gellan gum based physical hydrogels incorporating highly valuable endogen molecules and associating BMP-2 as bone formation platforms. *Carbohydrate Polym.* 2017;167:345–355. doi:10.1016/j.carbpol.2017.03.049